

Nondiffracting Supertoroidal Pulses: Optical “Kármán Vortex Streets”

Yijie Shen,^{1,*} Nikitas Papasimakis,¹ and Nikolay I. Zheludev^{1,2}

¹*Optoelectronics Research Centre & Centre for Photonic Metamaterials, University of Southampton, Southampton SO17 1BJ, United Kingdom*

²*Centre for Disruptive Photonic Technologies, School of Physical and Mathematical Sciences and The Photonics Institute, Nanyang Technological University, Singapore 637378, Singapore*

(Dated: April 13, 2022)

Recently introduced supertoroidal light pulses [Nat. Commun. 15, 5891 (2021)] are a family of space-time nonseparable freespace electromagnetic excitations with unique topological properties including skyrmionic field configurations, fractal-like patterns of singularities, and extended areas of energy backflow. Here we report nondiffracting supertoroidal pulses (ND-STPs), propagation-robust skyrmionic and vortex-ring field that endure the singular configurations over arbitrary propagation distances. Intriguingly, the field structure in of ND-STPs has a strong similarity with a von Kármán vortex street, a pattern of swirling vortices observed in fluid and gas dynamics that is responsible for the “singing” of suspended telephone lines in wind. We argue that ND-STPs are of interest as directed energy channels for telecom applications.

The topological properties of spatial light fields have been a subject of fascination and intense research interest over the last half century [1–3] with implications for light-matter interactions [4–6], nonlinear physics [7–9], spin-orbit coupling [10–12], microscopy and imaging [13–15], metrology [16], and information transfer [17–19]. Light pulses can also be simultaneously structured in space and time domains [20–24]. Among them, the toroidal pulses are of particular interest as they can engage toroidal excitations in matter [24–26] and exhibit space-time nonseparability and isodiffraction [27–29]. As a recent generalization of toroidal pulses, the supertoroidal pulses (STPs) also exhibit striking topology including fractal-like singularities, vortex rings, energy backflows, and optical skyrmionic patterns [30, 31].

In this Letter, we show that the transverse divergence of STPs can be tuned to archive nondiffracting supertoroidal pulses (ND-STPs). Intriguingly, the structure of an ND-STP resembles that of Kármán vortex street (KVS), staggered vortex arrays observed in fluid and gas dynamics [32], also previously observed in CW structured light fields [33–36].

STPs and ND-STPs originate from the “electromagnetic directed-energy pulse trains” (EDEPT) introduced by Ziolkowski [38]. Following Ziolkowski’s theory [38], the solutions are derived through a scalar generating function $f(\mathbf{r}, t)$ fulfilling the scalar wave equation, $(\nabla^2 - \frac{1}{c^2} \frac{\partial^2}{\partial t^2})f(\mathbf{r}, t) = 0$, where $\mathbf{r} = (r, \theta, z)$ represents spatial cylindrical coordinate, t is time, $c = 1/\sqrt{\varepsilon\mu}$ is the speed of light, and the ε and μ are the permittivity and permeability of medium. Here $f(\mathbf{r}, t) = f_0 e^{-s/q_3} (q_1 + i\tau)^{-1} (s + q_2)^{-\alpha}$, where f_0 is a normalizing constant, $s = r^2/(q_1 + i\tau) - i\sigma$, $\tau = z - ct$, $\sigma = z + ct$, q_1, q_2, q_3 are real positive parameters with units of length, and the real dimensionless parameter α must satisfy $\alpha \geq 1$, to ensure finite energy of the pulse [37, 38]. In order to retrieve the electromagnetic fields, we construct the Hertz potentials $\mathbf{\Pi}(\mathbf{r}, t) = \hat{\mathbf{n}}f(\mathbf{r}, t)$, where $\hat{\mathbf{n}}$ can be arbitrary vector

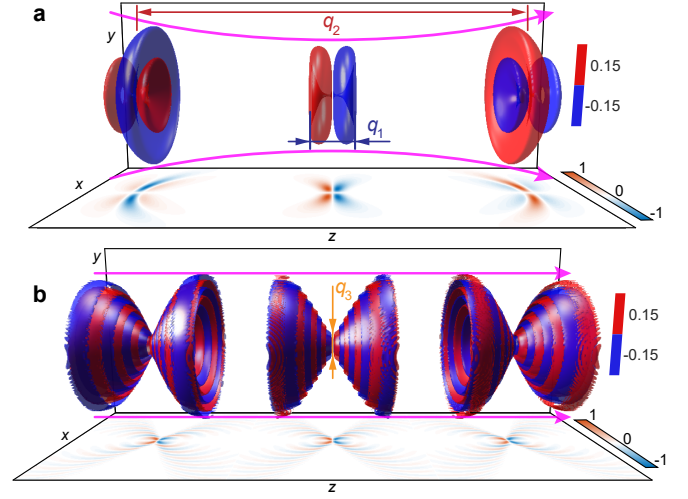


FIG. 1: An elementary toroidal pulse [37] (a) and a ND-STP (b): the isosurfaces with ± 0.15 amplitude level and the amplitude distributions on x - z plane at various times $t = 0, \pm q_2/(2c)$. Blue, red, and yellow arrows mark optical cycle (q_1), Rayleigh range (q_2), and transverse divergence (q_3), respectively. Parameters in simulation: $q_2/q_1 = 40$ for the toroidal pulse; $q_2/q_1 = 100$ and $q_3/q_1 = 1$ for the ND-STP. Purple arrows mark the propagation profile. See Supplementary Video 1 for the dynamic evolutions.

operator, and then the electromagnetic fields of transverse electric (TE) mode can be obtained by [37, 38]: $\mathbf{E}(\mathbf{r}, t) = -\mu_0 \frac{\partial}{\partial t} \nabla \times \mathbf{\Pi}$, $\mathbf{H}(\mathbf{r}, t) = \nabla \times (\nabla \times \mathbf{\Pi})$. If the Hertz potential is set as a transverse vortex vector field, i.e. $\hat{\mathbf{n}} = \nabla \times \hat{\mathbf{z}}$, the resulting electromagnetic field is an azimuthally polarized toroidal pulse [37], as shown in Fig. 1(a). The transverse magnetic (TM) mode can be obtained by exchanging electric and magnetic fields of the TE mode. If the Hertz potential is defined as $\hat{\mathbf{n}} = \hat{\mathbf{x}}$, the result is a linearly polarized pancake-like pulse (polarized along y -axis) [39]. In prior works, the conditions $q_1 \ll q_2$, $\alpha = 1$, and $q_3 \rightarrow \infty$ were assumed to generate various

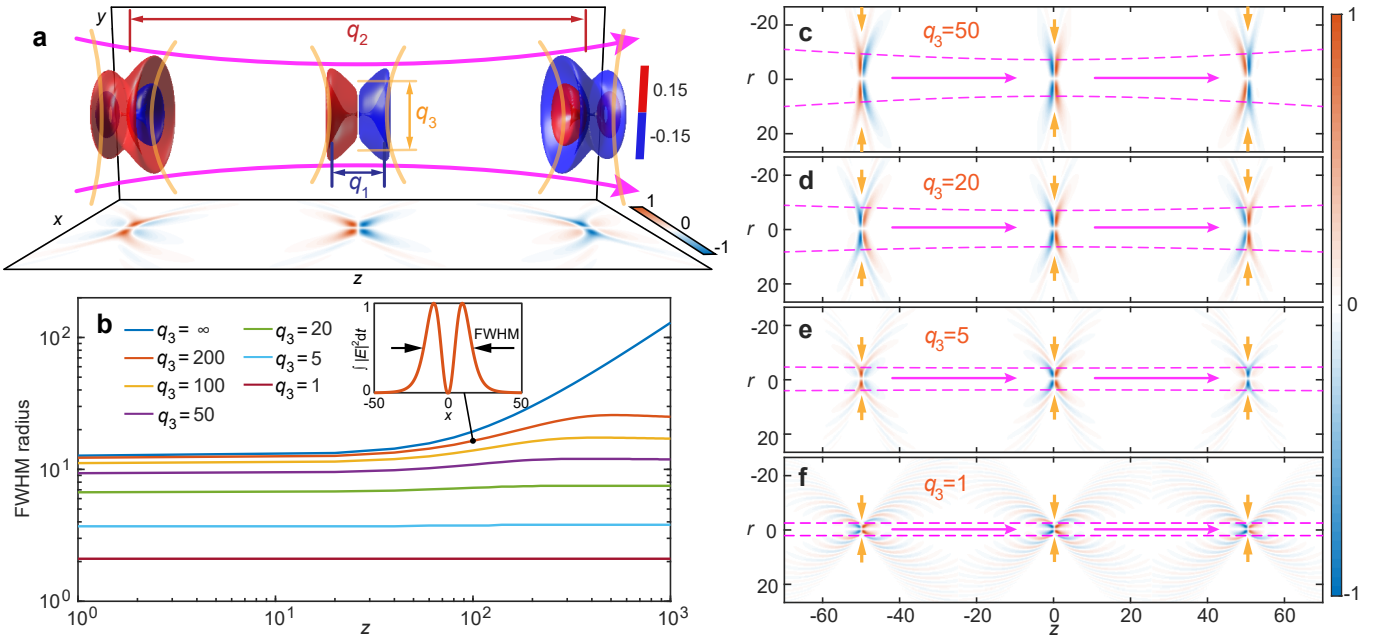


FIG. 2: (a) A characteristic example of a transversely divergent pulse with $q_3/q_1 = 20$, which is represented by electric field amplitude isosurfaces at levels ± 0.15 of the maximum field amplitude in three different moments in time $t = -q_2/(2c)$, 0 , $q_2/(2c)$. The presented case lies between the fundamental toroidal pulse [$q_3 \rightarrow \infty$; see Fig. Fig. 1(a)] and a ND-STP [$q_3 = q_1$; see Fig. 1(b)]. The transition from the former to the latter can be seen in Supplementary Video 1. (b) The evolution of pulse width in the transverse upon propagation for different q_3 values. The inset shows a 1D cross-section of the pulse intensity in the transverse plane, where the pulse width is quantified by the full width at half maximum (FWHM). (c-f) The spatiotemporal evolution of transversely divergent pulses with various q_3 values of 100, 20, 5, and 1, respectively. In each panel, the purple dashed lines mark the FWHM of the corresponding pulses. Unit of length: q_1 .

focused structured pulses [37, 39–42], where q_1 and q_2 determine the wavelength and the longitudinal divergence or Rayleigh length, $z_0 = q_2/2$ of the pulses, respectively, as marked in Fig. 1(a). The case of $\alpha \geq 1$ and $q_3 \rightarrow \infty$ was recently studied leading to the introduction of supertoroidal pulses [31]. In this work, we explore STPs with finite q_3 (see Supplementary Material for detailed derivation). A characteristic example of such a pulse with $q_3 = q_1$ and $\alpha = 1$ is plotted in Fig. 1(b). Here, q_3 defines the degree of transverse divergence: with decreasing value of q_3 the pulse envelope is gradually squeezed into a dumbbell-like shape and eventually becomes nondiffracting for $q_3 = q_1$ and $\alpha = 1$, fulfilling the definition of nondiffraction $|E(r, \theta, z, t)| = |E(r, \theta, z + \Delta z, t + \Delta z/v)|$ [43], where Δz is a given propagation distance and v is group velocity of the wave here $v = c$, see Supplementary for the proof.

The evolution of the pulse from diffracting to nondiffracting is illustrated in Fig. 2. An intermediate case of a weakly-diffracting supertoroidal pulse in terms of q_1 , q_2 , and q_3 , is presented Fig. 2(a). To illustrate the dependence of the (non)diffracting nature of the pulse on q_3 , we calculate the z -dependent full width at half maximum (FWHM) radius of the transverse intensity pattern of the STPs with $q_2 = 100q_1$ and q_3 varying from infinity to q_1 , for propagation distances from focus to $z = 10^3q_1$,

see Fig. 2(b). In the extreme case of $q_3 \rightarrow \infty$ (fundamental toroidal light pulse), the FWHM of the pulse follows a hyperbolic trajectory similar to a conventional focused Gaussian beam [37]. With decreasing q_3 , the divergence becomes weaker and the pulse approaches a nondiffracting state for $q_3 \leq 5q_1$. Figures 2(c)–2(f) show the spatiotemporal evolution upon propagation for toroidal pulses with different q_3 values. Here, decreasing q_3 , results in a faster spatiotemporal evolution of the cycle structure of the pulse (see Supplementary Video 1), due to its increasingly complex shape. When the q_3 value is decreased further to q_1 , then the pulse becomes X-shaped. Note that q_3 can be an arbitrarily small positive real number and can take values smaller than q_1 , in which case the pulse remains nondiffracting and becomes further squeezed. Figure 1(b) plots the special case of $q_3 = q_1$, where the X-shape reveals the conical structure in space, accommodating multiple cycles along the conical surface. Upon propagation, the cycle structure keeps evolving on the conical surface akin to a breather (see Supplementary Video 1). Note that similar X-type nondiffracting pulses have been considered previously both theoretically and experimentally and are typically termed Bessel-X pulses [44–46]. However, previous works focused on scalar long-pulses within the slowly-varying amplitude envelope approximation. Here, our

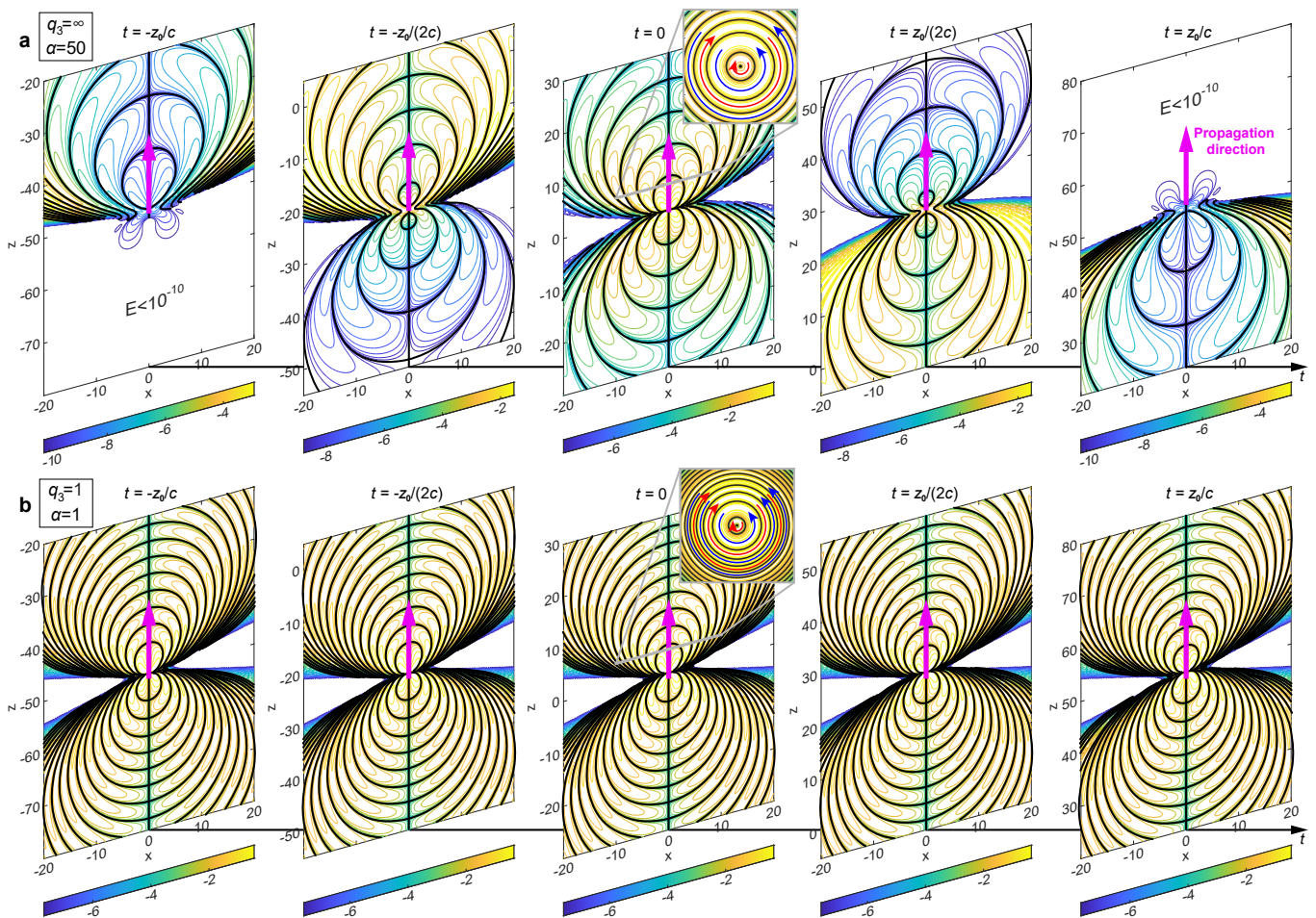


FIG. 3: The singular structures of electric field evolving with propagation versus the time for a focused supertoroidal pulse (a) and a ND-STP (b): each panel presents an isoline plot of the logarithm of the electric field of the pulse in the x - z plane at a given time. The singularities are highlighted by bold black lines. Unit of length: q_1 . See Supplementary Video 2 for the dynamic evolutions of figures (a) and (b), and other general cases with different parameters, respectively.

ND-STPs are few-cycle, space-time nonseparable with nontrivial electromagnetic toroidal topology lacking in the Bessel-X pulses. A typical example involves the intriguing skyrmions and KVS structures is discussed in this work.

The emergence of ND-STPs allows us to explore intriguing topological optical effects. In our recent work, we showed that supertoroidal pulses exhibit a complex topology (controlled by the parameter α), including self-similar fractal-like patterns, matryoshka-like singularity arrays, skyrmions, and areas of energy backflow [31]. Here, we show that such topological structures are also present in nondiffracting supertoroidal pulses. However, whereas in the former case, the self-similar topological structures were only instantaneously observed at focus, in the ND-STP, they can be observed over arbitrarily long distances [see example in Fig. 3(b)]. For instance, we have shown in our previous work that STPs exhibit a complex topology that evolves rapidly upon pulse propagation with elements of self-similarity con-

sisting of concentric matryoshka-like spherical shells over which the electric field vanishes [see Fig. 3(a)]. Similar propagation-robust fractal-like topological structures also exist in the ND-STP [see Fig. 3(b)] and persist upon pulse propagation (see also Supplementary Video 2).

The complex topology of the ND-STPs manifests also in the magnetic field distribution. Figure 4(a) shows the magnetic field distribution of a ND-STP with $q_2/q_1 = 100$ and $q_3/q_1 = 1$ at $t = 0$. The magnetic field includes both radial and longitudinal components resulting in vector singularities of vortex and saddle types. The saddle-type singularities are distributed along the propagation axis, while the vortices trace an off-axis trajectory, see Fig. 4(a1). Such a singularity distribution induces multiple electromagnetic skyrmions at transverse planes of the pulse, see Fig. 4(a2). In contrast to the propagating electromagnetic skyrmions in prior works that only exist around beam focus and collapse rapidly upon propagation [31, 47, 48], here in the ND-STP, the skyrmions persist upon propagation with their topological texture

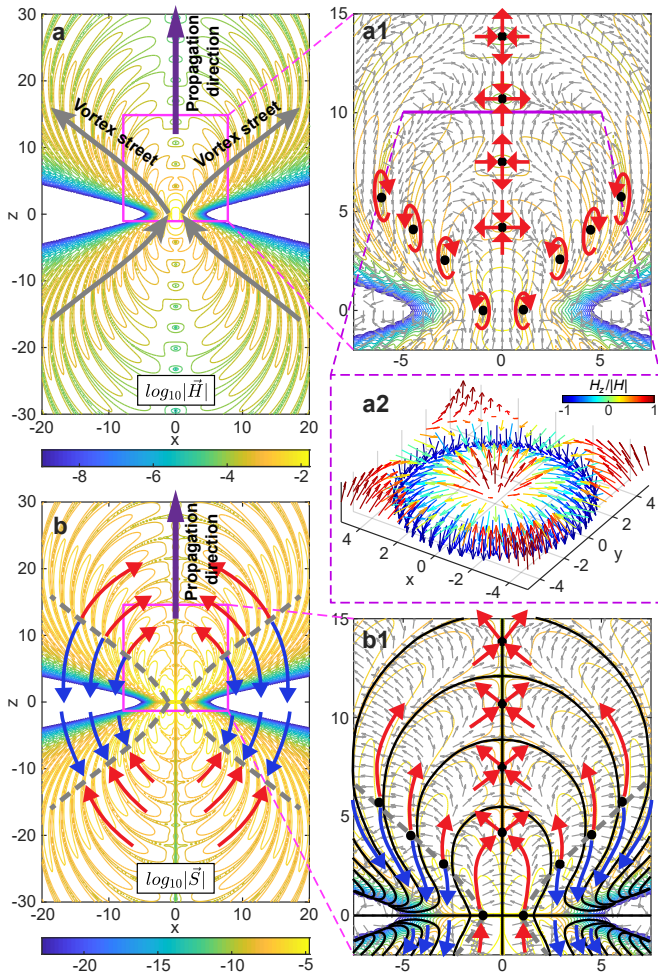


FIG. 4: Magnetic field **(a)** and Poynting vector **(b)** distributions of a ND-STP with $q_2/q_1 = 100$ and $q_3/q_1 = 1$ at $t = 0$. The contours show the logarithm of the modulus of the corresponding vectors. **(a1)** A zoom-in of the magnetic field with the arrow plot showing the vector distribution, the black dots referring to the singularities, and surrounding red arrows marking the type of the vector singularities (vortex and saddle) serving as guide to the eye. **(a2)** Arrow plot showing a skyrmionic structure of magnetic field in the transverse (x - y) plane at $z = 10$ (indicated by the purple solid line in **(a1)**). **(b1)** A zoom-in of the Poynting vector field, where the arrow plot corresponds to the vector distribution, solid black lines and dots mark the zeros of the Poynting vector, red and blue arrows indicate areas with forward and backward energy flow, respectively. Unit of length: q_1 .

exhibiting a periodic behaviour alternating between four different skyrmion types (combination of opposite two polarities and two helical angles), see Supplementary Video 3.

Figure 4**(b)** shows the Poynting vector field distribution of the ND-STP, which possesses layered energy forward-flow and backflow structures, see Fig. 4**(b1)**. Interestingly, energy transport is mediated by the vortex arrays of the magnetic field. Vortices on the front half

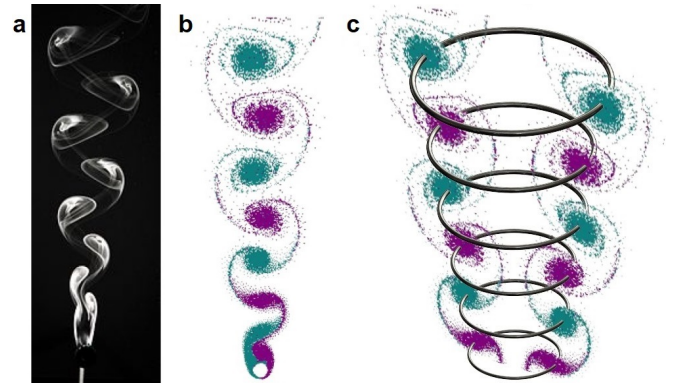


FIG. 5: **(a)** Visualization of a KSV behind a cylinder in air, where the flow is visualized by releasing glycerol vapour in the air near the cylinder. **(b)** Simulation of a 2D KSV, where the right- and left-handed vortices were highlighted by purple and cyan, respectively. **(c)** Artistic impressions of a vortex-ring street analogue to the structure of magnetic field of a ND-STP.

of the pulse act as energy sources, whereas the vortices in the rear half behave as sinks. In between sources and sinks, we observe areas of extended backflow. In areas of high intensity, energy flows primarily forward, ensuring the propagation of the pulse.

Moreover, we observe that the vortex arrays exhibited by the ND-STPs form a striking trail of two-vortex clusters (with opposite circulations, namely a vortex dipole) propagating in a periodic staggered manner, evocative of the KVS structure [Fig. 5**(a)**]. In fluid dynamics, a KVS is such a classic pattern of swirling vortices caused by a nonlinear process of vortex shedding, which refers to the unsteady separation of flow of a fluid around blunt bodies. Vortex-street-like optical fields were reported previously in stationary optical fields exhibiting phase vortex patterns [33–36]. In contrast, here we observe KVS-like structures in propagating electromagnetic spatiotemporal pulses in linear regime. In fluid dynamics, a KVS is a pattern of repeating swirling vortices constructed in the flow velocity field, whilst in our optical analogy, the KVS pattern is constructed by the electric or magnetic field of ND-STPs. Moreover, whereas KVS in fluid dynamics is a nonlinear phenomenon, here we show that similar effects can be observed in a linear system. The analogy between KVS in fluid flows and ND-STPs can be drawn further by considering for instance the motion of electrons along the vortex streets of a TM ND-STP or the propagation of superorbital pulses in nonlinear media. Finally, note that while the KVS is usually demonstrated in 2D [Fig. 5**(b)**], here the KVS in ND-STP corresponds to a 3D set of vortex rings, due to the cylindrical symmetry [Fig. 5**(c)**].

ND-STPs are vector polarized, space-time nonseparable pulses and as such they can be generated by spatially gradient metasurfaces, similarly to the toroidal pulses discovered by Helwarth and Nouchi [24, 37]. Of particu-

lar importance here is the relation between the size of the generating metasurface (aperture) and the distance over which the generated pulses propagate without diffraction. We have shown that in contrast to the well known Bessel beams, the field of the ND-STPs is exponentially confined (see Supplementary). We argue that the latter is less sensitive to the metasurface size and thus practical implementations of the latter remain closer to their ideal form.

In conclusion, we demonstrate nondiffracting toroidal pulses. Importantly, the sophisticated vector field configuration of ND-STPs induce robust topological structures including fractal-like singularities, skyrmions, vortex rings, and energy backflows, all of which can stably propagate at an infinitely long distance. Due to its propagation-robust topology, the ND-STP acts as a spectacular display of striking trail of staggered electromagnetic vortex dipole arrays with stable propagation, evocative of the classic KVS. The ND-STPs and optical KVSs unveil intriguing analogies between fluid transport and flow of energy in structured light. In particular, the robust topological structure of ND-STPs that remains invariant upon propagation could be used for long-distance information transfer encoded in the topological features of the pulses. Finally, we anticipate that ND-STPs will inspire potential applications such as light-matter interactions, superresolution microscopy, telecommunications, remote sensing and lidar.

Acknowledgments. The authors acknowledge the supports of the MOE Singapore (MOE2016-T3-1-006), the UKs Engineering and Physical Sciences Research Council (grant EP/M009122/1, Funder Id: <http://dx.doi.org/10.13039/501100000266>), the European Research Council (Advanced grant FLEET-786851, Funder Id: <http://dx.doi.org/10.13039/501100000781>), and the Defense Advanced Research Projects Agency (DARPA) under the Nascent Light Matter Interactions program.

* Electronic address: y.shen@soton.ac.uk

- [1] Nye, J. F. & Berry, M. V. Dislocations in wave trains. In *A Half-Century of Physical Asymptotics and Other Diversions: Selected Works by Michael Berry*, 6–31 (World Scientific, 1974).
- [2] Berry, M. Making waves in physics. *Nature* **403**, 21–21 (2000).
- [3] Dennis, M. R., O’Holleran, K. & Padgett, M. J. Singular optics: optical vortices and polarization singularities. *Progress in optics* **53**, 293–363 (2009).
- [4] Bao, C., Tang, P., Sun, D. & Zhou, S. Light-induced emergent phenomena in 2d materials and topological materials. *Nature Reviews Physics* 1–16 (2021).
- [5] Ozawa, T. *et al.* Topological photonics. *Reviews of Modern Physics* **91**, 015006 (2019).
- [6] Malinauskas, M. *et al.* Ultrafast laser processing of materials: from science to industry. *Light: Science & Applications* **5**, e16133–e16133 (2016).
- [7] Luu, T. T. *et al.* Extreme ultraviolet high-harmonic spectroscopy of solids. *Nature* **521**, 498–502 (2015).
- [8] Krogen, P. *et al.* Generation and multi-octave shaping of mid-infrared intense single-cycle pulses. *Nature Photonics* **11**, 222 (2017).
- [9] Shen, Y., Gao, G., Meng, Y., Fu, X. & Gong, M. Gain-phase modulation in chirped-pulse amplification. *Physical Review A* **96**, 043851 (2017).
- [10] Rego, L. *et al.* Generation of extreme-ultraviolet beams with time-varying orbital angular momentum. *Science* **364**, eaaw9486 (2019).
- [11] Dorney, K. M. *et al.* Controlling the polarization and vortex charge of attosecond high-harmonic beams via simultaneous spin-orbit momentum conservation. *Nature Photonics* **13**, 123–130 (2019).
- [12] Shen, Y. *et al.* Optical vortices 30 years on: Oam manipulation from topological charge to multiple singularities. *Light: Science & Applications* **8**, 1–29 (2019).
- [13] Davis, T. J. *et al.* Ultrafast vector imaging of plasmonic skyrmion dynamics with deep subwavelength resolution. *Science* **368** (2020).
- [14] Pu, T. *et al.* Unlabeled far-field deeply subwavelength topological microscopy (dstm). *Advanced Science* **8**, 2002886 (2021).
- [15] Pu, T., Ou, J.-Y., Papanikolaou, N. & Zheludev, N. I. Label-free deeply subwavelength optical microscopy. *Applied Physics Letters* **116**, 131105 (2020).
- [16] Yuan, G. H. & Zheludev, N. I. Detecting nanometric displacements with optical ruler metrology. *Science* **364**, 771–775 (2019).
- [17] Xie, Z. *et al.* Ultra-broadband on-chip twisted light emitter for optical communications. *Light: Science & Applications* **7**, 18001–18001 (2018).
- [18] Qiao, Z. *et al.* Multi-vortex laser enabling spatial and temporal encoding. *Photonix* **1**, 1–14 (2020).
- [19] Wan, Z. *et al.* Divergence-degenerated spatial multiplexing towards ultrahigh capacity, low bit-error-rate optical communications. *arXiv preprint arXiv:2110.08815* (2021).
- [20] Chong, A., Wan, C., Chen, J. & Zhan, Q. Generation of spatiotemporal optical vortices with controllable transverse orbital angular momentum. *Nature Photonics* **14**, 350–354 (2020).
- [21] Bliokh, K. Y. Spatiotemporal vortex pulses: Angular momenta and spin-orbit interaction. *Physical Review Letters* **126**, 243601 (2021).
- [22] Kondakci, H. E. & Abouraddy, A. F. Diffraction-free space-time light sheets. *Nature Photonics* **11**, 733–740 (2017).
- [23] Yessenov, M., Bhaduri, B., Kondakci, H. E. & Abouraddy, A. F. Weaving the rainbow: Space-time optical wave packets. *Optics and Photonics News* **30**, 34–41 (2019).
- [24] Zdagkas, A. *et al.* Observation of toroidal pulses of light. *arXiv preprint arXiv:2102.03636* (2021).
- [25] Papanikolaou, N., Fedotov, V., Savinov, V., Raybould, T. & Zheludev, N. Electromagnetic toroidal excitations in matter and free space. *Nature Materials* **15**, 263–271 (2016).
- [26] Raybould, T., Fedotov, V. A., Papanikolaou, N., Youngs, I. & Zheludev, N. I. Exciting dynamic anapoles with electromagnetic doughnut pulses. *Applied Physics Letters*

- 111, 081104 (2017).
- [27] Zdagkas, A., Papasimakis, N., Savinov, V. & Zheludev, N. I. Space-time nonseparable pulses: Constructing isodiffracting donut pulses from plane waves and single-cycle pulses. *Physical Review A* **102**, 063512 (2020).
- [28] Shen, Y., Zdagkas, A., Papasimakis, N. & Zheludev, N. I. Measures of space-time nonseparability of electromagnetic pulses. *Physical Review Research* **3**, 013236 (2021).
- [29] Shen, Y. & Rosales-Guzmán, C. Nonseparable states of light: From quantum to classical. *Laser & Photonics Reviews* (2022).
- [30] Zdagkas, A., Papasimakis, N., Savinov, V., Dennis, M. R. & Zheludev, N. I. Singularities in the flying electromagnetic doughnuts. *Nanophotonics* **8**, 1379–1385 (2019).
- [31] Shen, Y., Hou, Y., Papasimakis, N. & Zheludev, N. I. Supertoroidal light pulses as electromagnetic skyrmions propagating in free space. *Nature communications* **12**, 1–9 (2021).
- [32] von Kármán, T. *Aerodynamics. Selected topics in the light of their historical development* (Cambridge University Press, 1954).
- [33] Scheuer, J. & Orenstein, M. Optical vortices crystals: Spontaneous generation in nonlinear semiconductor microcavities. *Science* **285**, 230–233 (1999).
- [34] Molina-Terriza, G., Petrov, D. V., Recolons, J. & Torner, L. Observation of optical vortex streets in walking second-harmonic generation. *Optics letters* **27**, 625–627 (2002).
- [35] Molina-Terriza, G., Petrov, D. V. & Torner, L. Singular optics: Optical vortex streets. *Optics and Photonics News* **13**, 56–56 (2002).
- [36] Shen, Y., Wan, Z., Fu, X., Liu, Q. & Gong, M. Vortex lattices with transverse-mode-locking states switching in a large-aperture off-axis-pumped solid-state laser. *JOSA B* **35**, 2940–2944 (2018).
- [37] Hellwarth, R. & Nouchi, P. Focused one-cycle electromagnetic pulses. *Physical Review E* **54**, 889 (1996).
- [38] Ziolkowski, R. W. Localized transmission of electromagnetic energy. *Physical Review A* **39**, 2005 (1989).
- [39] Feng, S., Winful, H. G. & Hellwarth, R. W. Spatiotemporal evolution of focused single-cycle electromagnetic pulses. *Physical Review E* **59**, 4630 (1999).
- [40] Feng, S., Winful, H. G. & Hellwarth, R. W. Gouy shift and temporal reshaping of focused single-cycle electromagnetic pulses. *Optics Letters* **23**, 385–387 (1998).
- [41] Lekner, J. Localized electromagnetic pulses with azimuthal dependence. *Journal of Optics A: Pure and Applied Optics* **6**, 711 (2004).
- [42] Lekner, J. Helical light pulses. *Journal of Optics A: Pure and Applied Optics* **6**, L29 (2004).
- [43] Hernández-Figueroa, H. E., Zamboni-Rached, M. & Recami, E. *Non-diffracting waves* (John Wiley & Sons, 2013).
- [44] Saari, P. & Reivelt, K. Evidence of x-shaped propagation-invariant localized light waves. *Physical Review Letters* **79**, 4135 (1997).
- [45] Besieris, I. M. & Shaarawi, A. M. (2+ 1)-dimensional x-shaped localized waves. *Physical Review E* **72**, 056612 (2005).
- [46] Bowlan, P. *et al.* Measuring the spatiotemporal field of ultrashort bessel-x pulses. *Optics letters* **34**, 2276–2278 (2009).
- [47] Shen, Y. Topological bimeronic beams. *Optics Letters* **46**, 3737–3740 (2021).
- [48] Shen, Y., Martínez, E. C. & Rosales-Guzmán, C. Generation of optical skyrmions with tunable topological textures. *ACS Photonics* **9**, 296–303 (2022).